Current Biology 23, 307–311, February 18, 2013 ©2013 Elsevier Ltd All rights reserved http://dx.doi.org/10.1016/j.cub.2012.12.040

Report

Real-Time Visualization of Neuronal Activity during Perception

Akira Muto,[1,2,4] Masamichi Ohkura,[3,4] Gembu Abe,[1] Junichi Nakai,[3,*] and Koichi Kawakami[1,2,*]
[1]Division of Molecular and Developmental Biology, National Institute of Genetics, 1111 Yata, Mishima, Shizuoka 411-8540, Japan
[2]Department of Genetics, The Graduate University for Advanced Studies (SOKENDAI), 1111 Yata, Mishima, Shizuoka 411-8540, Japan
[3]Brain Science Institute, Saitama University, 255 Shimo-Okubo, Sakura-ku, Saitama 338-8570, Japan

Summary

To understand how the brain perceives the external world, it is desirable to observe neuronal activity in the brain in real time during perception. The zebrafish is a suitable model animal for fluorescence imaging studies to visualize neuronal activity because its body is transparent through the embryonic and larval stages. Imaging studies have been carried out to monitor neuronal activity in the larval spinal cord and brain using Ca^{2+} indicator dyes [1–3] and DNA-encoded Ca^{2+} indicators, such as Cameleon [4], GFP-aequorin [5], and GCaMPs [6–12]. However, temporal and spatial resolution and sensitivity of these tools are still limited, and imaging of brain activity during perception of a natural object has not yet been demonstrated. Here we demonstrate visualization of neuronal activity in the optic tectum of larval zebrafish by genetically expressing the new version of GCaMP. First, we demonstrate Ca^{2+} transients in the tectum evoked by a moving spot on a display and identify direction-selective neurons. Second, we show tectal activity during perception of a natural object, a swimming paramecium, revealing a functional visuotopic map. Finally, we image the tectal responses of a free-swimming larval fish to a paramecium and thereby correlate neuronal activity in the brain with prey capture behavior.

Results and Discussion

How the brain perceives the external world precisely under ever-changing operational conditions is a fundamental question in neuroscience. We approach this question by directly observing the activity of neuronal ensembles during behavior and perception of a model vertebrate, the zebrafish. Zebrafish larvae start to capture and eat live bait at 4 days postfertilization (dpf), exhibiting a behavior called prey capture. The prey capture behavior comprises a sequence of stereotyped events, i.e., perception of prey, eye convergence [13], and approach swimming [14]. As a first step toward understanding the functional neural circuits in the brain that control prey capture behavior, we aimed to visualize how neurons in the brain respond when a zebrafish larva perceives a swimming paramecium.

Previously, we developed GCaMP, an engineered GFP that increases fluorescence upon increase of cellular Ca^{2+} concentration [15], and generated an improved version GCaMP-HS to image the activity of spinal motor neurons during spontaneous contractions of a zebrafish larva [8]. However, we found that the sensitivity of GCaMP-HS was not high enough to image the visual system during perception of a natural object (data not shown). Therefore, we introduced amino acid substitutions into GCaMP-HS, tested their activities, and developed a new version, which we named GCaMP7a (see Figure S1A available online). We constructed UAS:GCaMP7a transgenic zebrafish carrying a codon-optimized GCaMP7a gene downstream of the Gal4 binding sequence UAS to express GCaMP7a under the control of a Gal4 driver line [16]. Then, to express GCaMP7a in the visual system, we performed a genetic screen using a *Tol2* transposon-mediated gene trap approach and identified gSA2AzGFF49A transgenic fish that expressed the Gal4FF transactivator in the optic tectum (Figures 1 and S1B). The gSA2AzGFF49A fish carried a single-copy integration of the gene trap construct within the *dlg2* (*discs large homolog 2*) gene (chapsyn-110, PSD-93), which is known to mediate clustering of ion channels at postsynaptic sites [17] (Figure S1C). We compared the performance of GCaMP7a with that of GCaMP-HS by mating gSA2AzGFF49A fish to UAS:GCaMP7a or UAS:GCaMP-HS fish. We demonstrated spontaneous neuronal activities in the tectum at single-cell resolution using a gSA2AzGFF49A; UAS:GCaMP7a double-transgenic larva at 3 dpf (Figure 1; Movie S1). Fluorescence changes detected with GCaMP7a were approximately 3.2-fold greater than those detected with GCaMP-HS (Figure S1D).

To analyze the tectal response to a visual stimulus, we placed a 3.5-inch LCD display to one side of the gSA2AzGFF49A; UAS:GCaMP7a larva and projected a spot with a diameter of ~13° on the display (Figure 2A). First, we analyzed tectal responses to appearance (ON) and disappearance (OFF) of the spot. In response to ON and OFF of the spot, Ca^{2+} transients were detected in the neuropil area, where the dendrites of tectal neurons form synapses with axons of retinal afferents (Figures 2B and 2C; Movie S2). ON and OFF subtypes of retinal cells were reported previously in zebrafish [18]. We showed that tectal cells responded to ON and OFF signals as well. Second, the spot was moved along the display in the anterior-to-posterior (A-to-P) and dorsal-to-ventral (D-to-V) directions. Ca^{2+} signals in the neuropil area of the tectum moved in A-to-P and D-to-V directions, respectively, in accordance with the movement of the spot, thus revealing visuotopy. Also, six tracks of the moving spot on the display were recapitulated on the neuropil area (Figures 2D and 2E). The cortical magnification factor was defined as the scaling factor that relates a distance in the visual field to the cortical distance [19]. We calculated the magnification factor (MF) by dividing the width of six tracks of Ca^{2+} signals on the neuropil by the visual angle corresponding to the width of six tracks of the moving spot on the display. We found that the vertical (D-to-V direction) MF was significantly larger than the horizontal (A-to-P direction) MF (vertical MF: 1.23 ± 0.17 μm/degree; horizontal MF: 0.62 ± 0.06 μm/degree; p = 0.033; paired

[4]These authors contributed equally to this work
*Correspondence: jnakai@mail.saitama-u.ac.jp (J.N.), kokawaka@nig.ac.jp (K.K.)

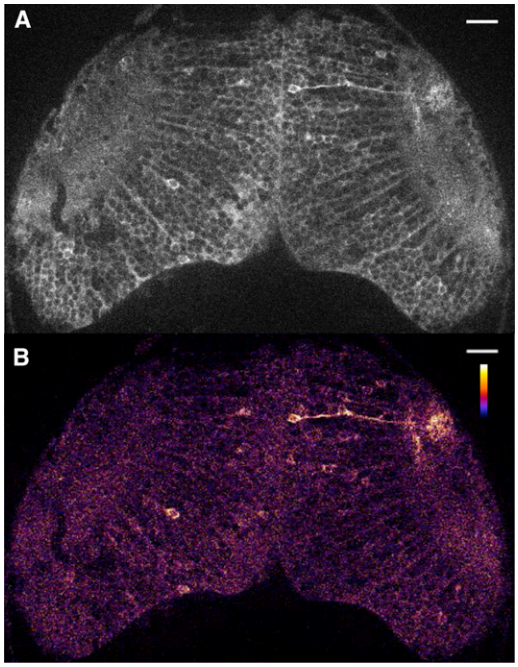

Figure 1. Spontaneous Neuronal Activity in the Optic Tectum in a Zebrafish Larva

(A) UAS:GCaMP7a fish were mated to gSA2AzGFF49A fish that expressed Gal4FF in the tectum. A double-transgenic larva at 3 dpf was embedded in agarose and imaged with a confocal microscope. A single raw image of the fluorescence intensity extracted from a time-lapse movie is shown (see Movie S1).

(B) The ratiometric image of (A) was created and pseudocolored to reveal the fluorescence change in the cell body and axon neurite of a single neuron. Scale bars represent 20 μm.

t test; n = 3), similar to those calculated for the mouse visual system [20]. Third, a spot was moved in the D-to-V and V-to-D directions, or P-to-A and A-to-P directions (Figures 2F–2J). Ca^{2+} transients detected in the cell bodies in D-to-V and P-to-A were merged with V-to-D and A-to-P, respectively, and single tectal neurons that responded selectively to the movement of only one direction were identified (Figures 2H and 2K). The presence of direction-selective neurons had been described previously by labeling of tectal cells with a Ca^{2+} indicator dye [3]. Our present method enabled identification of single direction-selective neurons in genetically tagged neurons. Overall, these results indicate that the temporal and spatial resolution of our present method are sensitive enough to detect neuronal activities in the tectum evoked by a small visual stimulus.

To examine the neuronal activity during perception of a natural object, we placed a live paramecium near the head of an immobilized gSA2AzGFF49A;UAS:GCaMP7a larva at 7 dpf. Ca^{2+} signals evoked by the paramecium were clearly detected in the neuropil area and the cell bodies of the

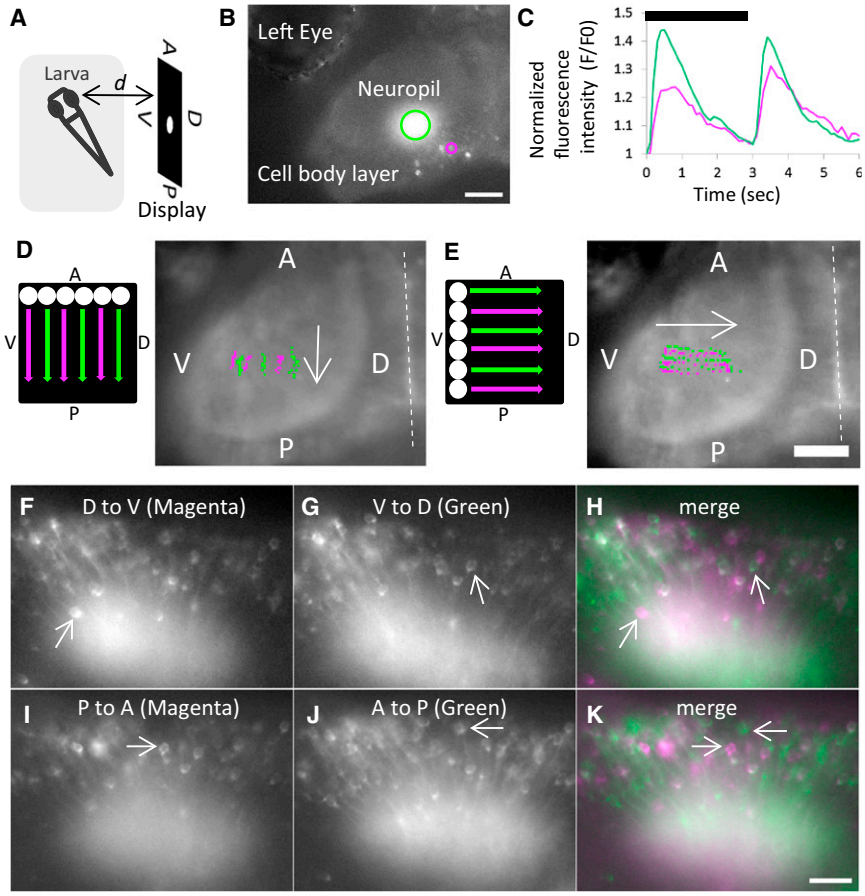

Figure 2. Tectal Responses to Visual Stimuli

(A) The recording setup, with the directions of the spot stimulus indicated on a display: A, anterior; P, posterior; D, dorsal; V, ventral. *d*, distance.

(B and C) ON and OFF responses in the optic tectum of a 6 days postfertilization (dpf) larva.

(B) Ca^{2+} signals detected in the neuropil (green) and cell body (magenta). Scale bar represents 50 μm.

(C) Normalized fluorescence intensity (F/F_0) in the neuropil (green) and cell body (magenta) was increased 0.4–0.5 s after ON and OFF of a spot on the display (Movie S2). The black bar indicates duration (3 s) of appearance (ON) of a spot. *d* = 15 mm.

(D and E) Visuotopic responses in the neuropil of a 7 dpf larva. A spot was moved along the display in the A-to-P (D) and V-to-D (E) directions at a speed of 13.4 mm/s for 1.6 s to create six tracks in parallel. The tracks are colored in magenta and green alternately. The area of Ca^{2+} signals on the neuropil in each frame (10 frames/s) was defined by setting the threshold manually, and the center of mass was plotted and colored in accordance with the color of the track. The Ca^{2+} signals moved in the A-to-P (D) and V-to-D (E) directions (indicated by arrows), and their movements recapitulated six tracks on the neuropil. Dashed lines indicate the midline of the larva. Scale bar represents 50 μm. *d* = 20 mm.

(F–K) Identification of direction-selective neurons in the optic tectum of a 5 dpf larva.

(F and G) A spot was moved along the D-V axis of the display to create six tracks (with a width of 21.45 mm) in the D-to-V (F) or V-to-D (G) directions.

(I and J) A spot was moved along the A-P axis of the display to create four tracks (with a width of 14.3 mm) in the P-to-A (I) and A-to-P (J) directions. Cells responding to D-to-V (F) and P-to-A (I) were colored in magenta, and cells responding to V-to-D (G) and A-to-P (J) were colored in green.

(H and K) (F) and (I) were merged with (G) and (J), respectively, and direction-selective neurons were identified (arrows). Scale bar represents 25 μm. *d* = 15 mm.

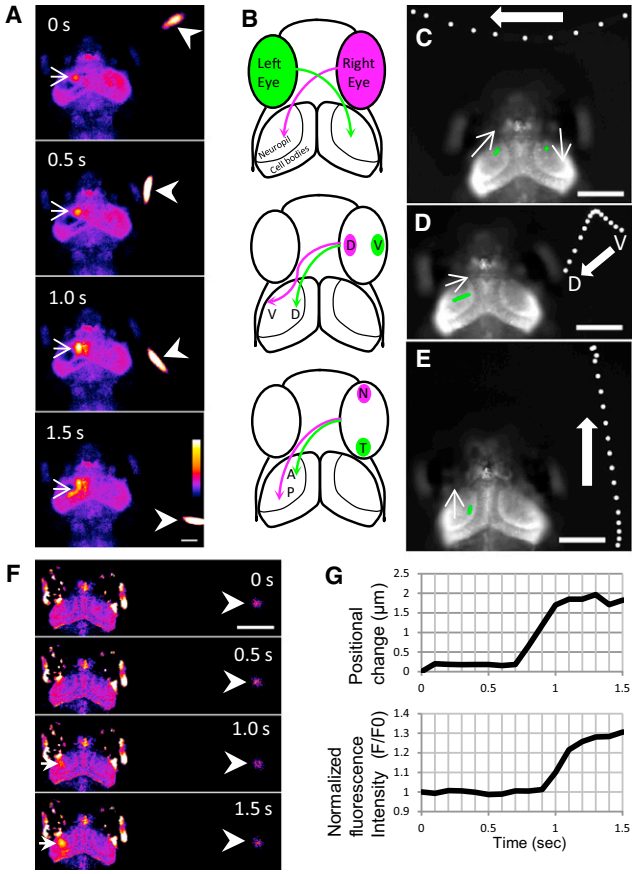

Figure 3. Tectal Responses during Perception of a Swimming Paramecium

(A) In response to a swimming paramecium (arrowheads), Ca^{2+} transients (arrows) were detected in the neuropil and cell bodies of the left tectum of a 7 dpf larva embedded in agarose (Movie S3). Ratio images were created and pseudocolored. Scale bar represents 100 μm.

(B) Retinotopic projections of the retinal ganglion cell axons: D, dorsal; V, ventral; N, nasal; T, temporal; A, anterior; P, posterior.

(C–E) Functional visuotopy (Movie S3). White spots indicate the positions of a paramecium, moving in the indicated directions. Green spots indicate the positions of Ca^{2+} signals in the neuropil. Scale bars represent 100 μm.

(C) A paramecium moved from the right to left hemifield, and the Ca^{2+} signal moved from the left to right tectum.

(D) A paramecium and Ca^{2+} signals moved from ventral to dorsal.

(E) A paramecium and Ca^{2+} signals moved from posterior to anterior.

(F and G) Ca^{2+} signals in the tectum of a 7 dpf larva evoked by motion of a paramecium (Movie S4).

(F) Ratio images of Ca^{2+} signals (arrows) detected when a paramecium (arrowheads) started to move. Scale bar represents 250 μm.

(G) Graph plots of Ca^{2+} signals and positional changes of the paramecium. The paramecium started to move at 0.7 s (upper graph), and the fluorescence change was detectable after 0.9 s (lower graph).

tectum (Figure 3A; Movie S3). The functional visuotopic map revealed by the present imaging is consistent with the retinotopic map derived from anatomical studies [21, 22] (Figure 3B). Namely, when a paramecium moved from the right to left hemifield, from ventral to dorsal, or from posterior to anterior, Ca^{2+} transients moved from the left to right tectum, from the center (ventral) to margin (dorsal), or from posterior to anterior in the neuropil area of the contralateral tectum, respectively (Figure 3C–3E; Movie S3). We found that the zebrafish larval visual system is capable of responding to a moving paramecium, but not to a motionless one. In cases where a motionless paramecium stayed close to the eye of the larva, Ca^{2+} signals were not detected in the contralateral tectum. However, when the paramecium started to move, the tectal neurons were activated (Figures 3F and 3G; Movie S4). Thus, the present study demonstrates that a moving object can generate signals on the tectum continuously.

Finally, we aimed to visualize the neuronal activity during prey capture behavior. For this purpose, we placed a free-swimming larva at 5 dpf with a paramecium in a small dish under an objective lens with low magnification. Because the larva swims in an intermittent manner, Ca^{2+} signals could be detected during pauses between swimming bouts. In this manner, Ca^{2+} signals, fish behaviors, and a paramecium could be simultaneously observed (Figures 4A–4D; Movie S5). Fish larvae occasionally performed a prey capture behavior, as judged by eye convergence and approach swimming toward the paramecium (Figure 4D). We mapped and analyzed positions of the Ca^{2+} signals on the tectum evoked by the paramecium. The total Ca^{2+} signals detected during imaging were mapped at position 0 to 1 along the anteroposterior axis in the neuropil area of the tectum (mean ± SD; 0.60 ± 0.20, 1,768 frames in the course of 18 sets of recording were analyzed) (Figure 4E). In contrast, the Ca^{2+} signals immediately followed by prey capture behavior were mapped between positions 0.2 and 0.42 (mean ± SD; 0.28 ± 0.09, 18 frames out of the 1,768 frames were analyzed) of the total tectal length from the anterior end (Figure 4F). Thus, Ca^{2+} signals preceding prey capture behavior were located more anteriorly in the tectum ($p < 0.0001$), suggesting that activation of the anterior tectum may be functionally connected to a subsequent visuomotor pathway that induces eye convergence and approach swimming. The positions of the paramecia that evoked anterior activation were mapped in front of the larva as expected from the visuotopic map (Figure S2).

In this study, we demonstrated dynamic responses of tectal neurons during visual perception of a natural object and correlated tectal activity with prey capture in free-swimming fish. This approach should facilitate understanding of the functional neuronal circuits essential for prey capture behavior. Furthermore, because GCaMP7a can be expressed via the Gal4FF-UAS system, neuronal activities in other regions of the brain can also be imaged by selecting appropriate Gal4FF driver lines from the transgenic resource [23]; in fact, we could successfully image spontaneous activities of single neurons in the habenula and hindbrain in double-transgenic larvae carrying region-specific Gal4FF drivers (Movie S6). Thus, our system should enable real-time imaging of genetically tagged neurons in the brain that may control behavior and locomotion.

Experimental Procedures

The gSA2AzGFF49A;UAS:GCaMP7a double-transgenic zebrafish used for imaging were also homozygous for the *nacre* pigmentation mutation [24] to eliminate melanophores. For imaging, a microscope (AxioImager Z1, Zeiss) equipped with a cooled CCD camera (ORCA-R2, Hamamatsu Photonics) or with a confocal scanner unit (CSU-W1, Yokogawa Electric Corporation) and an EMCCD camera (iXon, Andor Technology) was used. Visual stimuli were created using MATLAB (The MathWorks) and Psychtoolbox (http://psychtoolbox.org/). Image processing was performed with ImageJ (http://imagej.nih.gov/ij/). For more details, see Supplemental Experimental Procedures.

This study was carried out in accordance with the Guide for the Care and Use of Laboratory Animals of the Institutional Animal Care and Use Committee (IACUC, approval identification number 24-2) of the National Institute of Genetics (NIG, Japan), which has an Animal Welfare Assurance

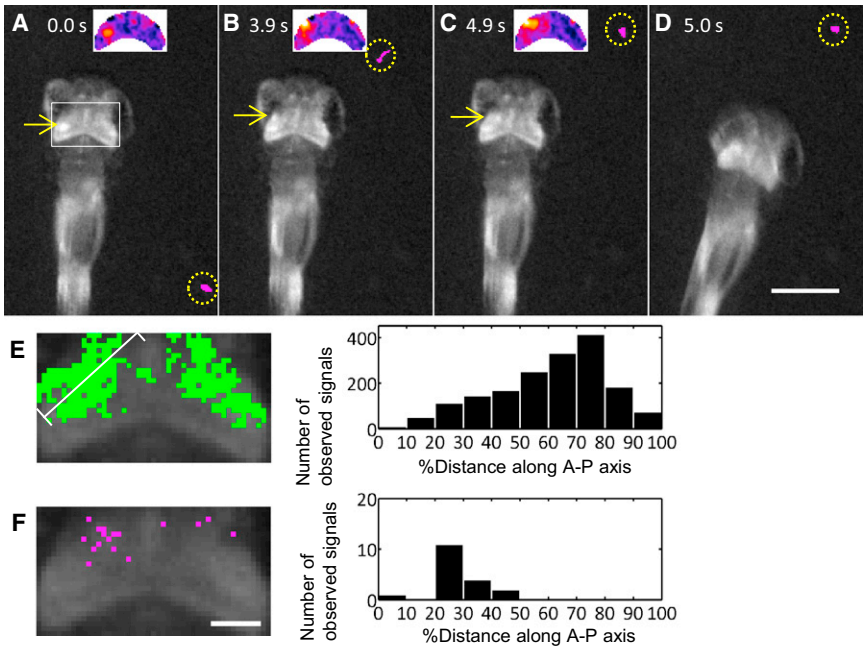

Figure 4. Tectal Responses of a 5 dpf Free-Swimming Larva during Perception of a Prey

(A–D) Ca^{2+} signals in the tectum and prey capture behavior (Movie S5).

(A–C) Ca^{2+} signals (arrows) were detected in the left tectum (arrows) when a paramecium moved from posterior to anterior on the right. Insets are pseudocolored ratio images.

(C and D) The fish changed its direction and started approach swimming. The swimming paramecium is colored in magenta and encircled by dotted lines.

(E) Left: positions of total Ca^{2+} signals observed on the tectal neuropil during the recording. Right: histogram of the Ca^{2+} signals' relative distances along the anteroposterior axis of the tectum.

(F) Left: positions of the Ca^{2+} signals observed in (C), one frame before the start of approach swimming. Right: histogram of the Ca^{2+} signals' relative distances. Scale bar represents 100 μm.

on file (assurance number A5561-01) at the Office of Laboratory Animal Welfare of the National Institutes of Health (NIH, USA).

Accession Numbers

The DNA Data Bank of Japan (DDBJ) accession number for GCaMP7a reported in this paper is AB775940.

Supplemental Information

Supplemental Information includes two figures, Supplemental Experimental Procedures, and six movies and can be found with this article online at http://dx.doi.org/10.1016/j.cub.2012.12.040.

Acknowledgments

We thank E. Stout for assistance with image analysis and A. Ito, Y. Kanebako, N. Mouri, M. Mizushina, and M. Suzuki for fish room maintenance. This work was supported by grants from the Mitsubishi Foundation (A.M.), the National BioResource Project, and the Ministry of Education, Culture, Sports, Science and Technology of Japan.

Received: November 30, 2012
Revised: December 23, 2012
Accepted: December 24, 2012
Published: January 31, 2013

References

1. Fetcho, J.R., and O'Malley, D.M. (1995). Visualization of active neural circuitry in the spinal cord of intact zebrafish. J. Neurophysiol. *73*, 399–406.
2. Friedrich, R.W., and Korsching, S.I. (1997). Combinatorial and chemotopic odorant coding in the zebrafish olfactory bulb visualized by optical imaging. Neuron *18*, 737–752.
3. Niell, C.M., and Smith, S.J. (2005). Functional imaging reveals rapid development of visual response properties in the zebrafish tectum. Neuron *45*, 941–951.
4. Higashijima, S., Masino, M.A., Mandel, G., and Fetcho, J.R. (2003). Imaging neuronal activity during zebrafish behavior with a genetically encoded calcium indicator. J. Neurophysiol. *90*, 3986–3997.
5. Naumann, E.A., Kampff, A.R., Prober, D.A., Schier, A.F., and Engert, F. (2010). Monitoring neural activity with bioluminescence during natural behavior. Nat. Neurosci. *13*, 513–520.
6. Sumbre, G., Muto, A., Baier, H., and Poo, M.M. (2008). Entrained rhythmic activities of neuronal ensembles as perceptual memory of time interval. Nature *456*, 102–106.
7. Del Bene, F., Wyart, C., Robles, E., Tran, A., Looger, L., Scott, E.K., Isacoff, E.Y., and Baier, H. (2010). Filtering of visual information in the tectum by an identified neural circuit. Science *330*, 669–673.
8. Muto, A., Ohkura, M., Kotani, T., Higashijima, S., Nakai, J., and Kawakami, K. (2011). Genetic visualization with an improved GCaMP calcium indicator reveals spatiotemporal activation of the spinal motor neurons in zebrafish. Proc. Natl. Acad. Sci. USA *108*, 5425–5430.
9. Ahrens, M.B., Li, J.M., Orger, M.B., Robson, D.N., Schier, A.F., Engert, F., and Portugues, R. (2012). Brain-wide neuronal dynamics during motor adaptation in zebrafish. Nature *485*, 471–477.
10. Akerboom, J., Chen, T.W., Wardill, T.J., Tian, L., Marvin, J.S., Mutlu, S., Calderón, N.C., Esposti, F., Borghuis, B.G., Sun, X.R., et al. (2012). Optimization of a GCaMP calcium indicator for neural activity imaging. J. Neurosci. *32*, 13819–13840.
11. Nikolaou, N., Lowe, A.S., Walker, A.S., Abbas, F., Hunter, P.R., Thompson, I.D., and Meyer, M.P. (2012). Parametric functional maps of visual inputs to the tectum. Neuron *76*, 317–324.
12. Wei, H.P., Yao, Y.Y., Zhang, R.W., Zhao, X.F., and Du, J.L. (2012). Activity-induced long-term potentiation of excitatory synapses in developing zebrafish retina in vivo. Neuron *75*, 479–489.
13. Bianco, I.H., Kampff, A.R., and Engert, F. (2011). Prey capture behavior evoked by simple visual stimuli in larval zebrafish. Front. Syst. Neurosci. *5*, 101.
14. McElligott, M.B., and O'Malley, D.M. (2005). Prey tracking by larval zebrafish: axial kinematics and visual control. Brain Behav. Evol. *66*, 177–196.
15. Nakai, J., Ohkura, M., and Imoto, K. (2001). A high signal-to-noise Ca^{2+} probe composed of a single green fluorescent protein. Nat. Biotechnol. *19*, 137–141.
16. Asakawa, K., Suster, M.L., Mizusawa, K., Nagayoshi, S., Kotani, T., Urasaki, A., Kishimoto, Y., Hibi, M., and Kawakami, K. (2008). Genetic dissection of neural circuits by Tol2 transposon-mediated Gal4 gene and enhancer trapping in zebrafish. Proc. Natl. Acad. Sci. USA *105*, 1255–1260.
17. Kim, E., Cho, K.O., Rothschild, A., and Sheng, M. (1996). Heteromultimerization and NMDA receptor-clustering activity of Chapsyn-110, a member of the PSD-95 family of proteins. Neuron *17*, 103–113.
18. Connaughton, V.P., and Nelson, R. (2000). Axonal stratification patterns and glutamate-gated conductance mechanisms in zebrafish retinal bipolar cells. J. Physiol. *524*, 135–146.

19. Daniel, P.M., and Whitteridge, D. (1961). The representation of the visual field on the cerebral cortex in monkeys. J. Physiol. *159*, 203–221.
20. Schuett, S., Bonhoeffer, T., and Hübener, M. (2002). Mapping retinotopic structure in mouse visual cortex with optical imaging. J. Neurosci. *22*, 6549–6559.
21. Stuermer, C.A. (1988). Retinotopic organization of the developing retinotectal projection in the zebrafish embryo. J. Neurosci. *8*, 4513–4530.
22. Baier, H., Klostermann, S., Trowe, T., Karlstrom, R.O., Nüsslein-Volhard, C., and Bonhoeffer, F. (1996). Genetic dissection of the retinotectal projection. Development *123*, 415–425.
23. Kawakami, K., Abe, G., Asada, T., Asakawa, K., Fukuda, R., Ito, A., Lal, P., Mouri, N., Muto, A., Suster, M.L., et al. (2010). zTrap: zebrafish gene trap and enhancer trap database. BMC Dev. Biol. *10*, 105.
24. Lister, J.A., Robertson, C.P., Lepage, T., Johnson, S.L., and Raible, D.W. (1999). nacre encodes a zebrafish microphthalmia-related protein that regulates neural-crest-derived pigment cell fate. Development *126*, 3757–3767.